Eur. Phys. J. B **10**, 119–129 (1999)

THE EUROPEAN PHYSICAL JOURNAL B

EDP Sciences

Correlations of conductance peaks and transmission phases in deformed quantum dots

R. Baltin[1], Y. Gefen[2], G. Hackenbroich[1,3,a], and H.A. Weidenmüller[1]

[1] Max Planck Institut für Kernphysik, Postfach 103980, 69029 Heidelberg, Germany
[2] Department of Condensed Matter Physics, The Weizmann Institute of Science, Rehovot 76100, Israel
[3] Universität GH Essen, Fachbereich 7, 45117 Essen, Germany

Received 17 July 1998

Abstract. We investigate the Coulomb blockade resonances and the phase of the transmission amplitude of a deformed ballistic quantum dot weakly coupled to leads. We show that preferred single-particle levels exist which stay close to the Fermi energy for a wide range of values of the gate voltage. These states give rise to sequences of Coulomb blockade resonances with correlated peak heights and transmission phases. The correlation of the peak heights becomes stronger with increasing temperature. The phase of the transmission amplitude shows lapses by π between the resonances. Implications for recent experiments on ballistic quantum dots are discussed.

PACS. 73.23.Hk Coulomb blockade; single-electron tunneling – 73.23.Ps Other electronic properties of mesoscopic systems – 73.40.Gk Tunneling

1 Introduction

Quantum dots have been intensively investigated both experimentally and theoretically [1] in recent years. In this paper, we present a theoretical study of the correlations of conductance peaks and of transmission phases that have been observed in recent experiments on quantum dots in the Coulomb blockade regime.

Quantum dots are small islands of electrons that are only a few hundred nanometers in size and typically contain a few hundred electrons. The spectrum of a quantum dot is determined by the Coulomb interaction of the electrons and by the external electrostatic confining potential. The confining potential and hence the size and shape of a quantum dot can be controlled by external gates. This makes quantum dots an ideal tool for studying the properties of finite systems of interacting fermions.

Experimentally, the spectra of quantum dots have been measured using optical (far-infrared) spectroscopy and/or transport experiments. In the latter case, the quantum dot is coupled *via* tunnel barriers to external leads. The conductance measured at a finite drain-source voltage reveals the excitation spectrum of the dot whereas the linear conductance yields the addition spectrum of the quantum dot. Both the excitation and the addition spectrum are dominated by the classical Coulomb blockade effect: large conductance peaks are observed when the dot potential is tuned in such a way that the number of electrons on the dot can fluctuate without any cost in energy. These peaks are nearly periodic in the gate voltage on the dot. At consecutive peaks the number of electrons on the dot changes by one. At values of the gate voltage located between the positions of the conductance peaks, electron transport through the dot requires a large charging energy. Hence, the current between conductance peaks is strongly suppressed, the remaining current being mostly due to virtual tunneling processes (co-tunneling regime) [2].

Typically, metallic quantum dots have such a large density of states that the Coulomb blockade oscillations can be described by classical theory which ignores the discreteness of the spectrum. The situation is different in semiconductor dots. Here, the mean single-particle level spacing Δ can be larger than the temperature kT. The regime $\Delta \gg kT, \Gamma$, where Γ is the strength of the coupling to the leads, is the resonant tunneling regime. In this regime, each conductance peak is mediated by a single quantum state of the dot. The peak height of the conductance resonance is a direct signature of the wave function of the resonant state.

Some years ago, Jalabert, Stone, and Alhassid developed a statistical theory of the Coulomb blockade resonances [3] in the resonant tunneling regime $\Delta \gg kT$. These authors assumed that the single-particle states of a quantum dot can be described as eigenstates of an ensemble of random matrices. This approach predicts a universal distribution of peak heights determined by the fundamental symmetries of the system, and no correlations for the peak heights of neighboring peaks.

[a] e-mail: hacken@theo-phys.uni-essen.de

The distribution of peak heights was investigated in two experiments [4,5]. Good agreement with the Porter-Thomas statistics of Random Matrix Theory (RMT) was found. Other quantities like the distribution of spacings between resonances [6] and particularly peak height correlations [5,10] showed deviations from the predictions of RMT[1].

Alhassid, Gökcedag and Stone [7] extended the statistical theory of the Coulomb blockade resonances to the regime where the resonant tunneling condition $\Delta \gg kT$ is not fully met. Then, a single conductance peak receives contributions from *several* single-particle states which lie in the vicinity of the Fermi energy, and correlations in the peak heights of adjacent resonances are expected to occur. In reference [5] significant correlations in the peak heights of 4–5 adjacent resonances were observed experimentally even for $\Delta > kT$. This question was analyzed further in a very recent experiment [10]. The authors of reference [10] found that the correlations increase with increasing temperature. In both experiments [5,10] the correlations exceed those predicted by RMT.

Even stronger correlations have been reported in experiments using a quantum dot embedded in an Aharanov-Bohm ring [11]. In this experiment where the lithographic shape of the dot was more regular than in reference [5,10], both peak heights and phases of the transmission amplitude could be measured. Strong correlations both in peak height and in phase within sequences of more than 10 resonances were found. As in references [10], temperature can be ruled out as the *only* source of correlations, and a mechanism different from and acting in addition to temperature must be the origin of these correlations.

In this paper we propose such a mechanism. Our model involves certain geometry-specific assumptions and is therefore restricted in generality and universality. Nevertheless it may still pertain to experiments on nearly integrable ballistic dots (*cf.* Sect. 3). Our mechanism is a synthesis of two approaches developed earlier [12,13]. In reference [12] a scenario was described for peak correlations at *vanishing temperature*. It was argued that deformation of the confining potential of the dot generically gives rise to avoided crossings of the single-particle levels on the dot. As a result of such crossings one and the same eigenstate of the dot may dominate a sequence of neighboring conductance peaks [12] and thereby cause correlations. Although several arguments in support of this mechanism were given [12], a quantitative study of the resulting correlations has not been presented yet. A different line of thought was pursued in reference [13]. That paper aimed at explaining the "phase lapse" observed in the experiment of reference [11] (a different theoretical discussion of the phase lapse was presented in Ref. [14]). It was shown [13] that the phase-lapse behavior as well as strong *finite temperature* correlations of conductance peaks arise if the dot supports one particularly well conducting state. This state would dominate a sequence of conductance peaks provided it remained within an energy interval of order kT around the Fermi energy.

[1] The deviations of the former from RMT may be due to the limitation of the constant interaction model for the Coulomb interaction [8]. It has also been suggested that deformations of the dot confining potential are involved [9] rather than a breakdown of RMT.

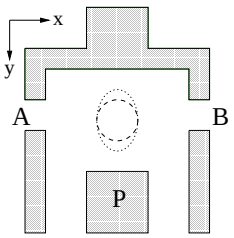

Fig. 1. A quantum dot (schematic). Electrons enter or leave the dot through the tunneling barriers A and B. The plunger gate P controls the number of electrons on the dot. Equipotential lines of the confining potential are shown for the isotropic (dashed) and deformed (dotted) case.

Here we study peak-height correlations and the transmission phase in quantum dots taking a deformed harmonic oscillator as a specific example. Using this model, we show that deformation of the confining potential leads to peak-height correlations, in keeping with the arguments of reference [12]. We identify those eigenstates of the quantum dot that are most strongly coupled to the external leads and which, therefore, support the bulk of the current through the dot. Peak-height correlations are strongest for sequences of resonances mediated by such states. We also investigate the influence of temperature on the correlations. As expected from the studies in reference [13], we find that temperature leads to a marked increase of the correlations. Combining the effect of deformation and of temperature, we obtain sequences of up to 30 conductance resonances with similar transmission phases and similar peak heights. We address the question whether this same mechanism might also account for the phase behavior observed in reference [11].

The paper is organized as follows: in the next section we introduce a model for a deformed quantum dot and describe how correlations can arise. In Section 3 we calculate the conductance with the help of a master equation. In Section 4 we investigate the transmission phase. This phase can be measured in Aharonov-Bohm type experiments containing a quantum dot. The last section gives a summary and a discussion of the limitations of our model.

2 The model

The confining potential of a quantum dot is often defined electrostatically in terms of a split gate. As depicted in Figure 1, this is an arrangement of electrodes on the surface of a heterostructure. When a negative bias is applied to the gates, the two-dimensional electron gas located some 100 nm or so beneath the electrodes will be depleted. The barriers through which electrons can tunnel between the leads and the dot are denoted by A and B. A voltage $V_{\rm g}$ applied to the plunger gate P controls

the chemical potential on the dot. A change of $V_{\rm g}$ not only changes the number of electrons on the dot but also distorts the confining potential of the two-dimensional electron gas in a substantial way, causing a deformation of the quantum dot [12].

We consider the standard Hamiltonian H for a quantum dot coupled to leads, containing the Hamiltonians $H^{\rm L}$ and $H^{\rm R}$ of the left and right leads, respectively, the Hamiltonian of the isolated quantum dot $H^{\rm D}$, and the Hamiltonian $H^{\rm T}$ for tunneling between the leads and the dot,

$$H = H^{\rm L} + H^{\rm R} + H^{\rm D} + H^{\rm T}, \tag{1}$$

$$H^{\rm L(R)} = \sum_k \epsilon_k^{\rm L(R)}\ a_k^{\rm L(R)\dagger} a_k^{\rm L(R)},$$

$$H^{\rm D} = \sum_n \epsilon_n c_n^\dagger c_n + \frac{1}{2} U\hat{N}(\hat{N}-1),$$

$$H^{\rm T} = \sum_{n,k} \left(V_{n,k}^{\rm L} a_k^{\rm L} c_n^\dagger + {\rm h.c.}\right) + \sum_{n,k} \left(V_{n,k}^{\rm R} a_k^{\rm R} c_n^\dagger + {\rm h.c.}\right).$$

Here, $\epsilon_k^{\rm L,R}$ and ϵ_n are the energies and $a_k^{\rm L,R}$ and c_n the annihilation operators for single-particle states in the leads and in the dot, respectively. For the Coulomb interaction on the quantum dot we use the constant interaction model with $\hat{N} = \sum_n n_n$ the number of electrons on the quantum dot. The tunneling matrix elements $V_{i,k}^{\rm L(R)}$ involve the overlap of wave functions in the leads and in the dot and are given below.

We model the confining potential as an anisotropic harmonic oscillator potential. A harmonic potential has been used previously in studies of quantum dots [15] and, at least for small dots, is believed to be a fair approximation to the true confining potential. Although we use a specific model, most of our conclusions apply to any sufficiently smooth confining potential for which the Hamiltonian is nearly integrable. Then, the transverse and longitudinal modes in the dot are nearly decoupled (*cf.* Eq. (2)). This condition is met when the matrix elements of the perturbation violating integrability are smaller than the mean single-particle level spacing. However, even mild disorder or boundary roughness violating this condition will modify our picture considerably.

The energy eigenvalues ϵ_n for the quantum numbers $n = (n_x, n_y)$ are given by

$$\epsilon_n = E(n_x, n_y) = \hbar\omega_x(n_x + \frac{1}{2}) + \hbar\omega_y(V_{\rm g})(n_y + \frac{1}{2}) - \alpha V_{\rm g} + E_0. \tag{2}$$

To describe the deformation, we assume that the oscillator frequency $\omega_y(V_{\rm g}) = \omega_x(1 - \gamma(V_{\rm g} - V_0))$ in the transverse direction y depends linearly on the gate voltage $V_{\rm g}$ while the frequency ω_x in the longitudinal x-direction is held fixed. The parameter α relates the overall depth of the dot's potential to the gate voltage. The constants E_0 and V_0 determine the number of electrons on the dot at zero deformation.

The dependence of the single-particle levels on the gate voltage is shown in Figure 2. The shell structure of the isotropic harmonic oscillator ($V_{\rm g} = V_0$) is clearly visible. It survives for small values of $V_{\rm g}$ but is eventually destroyed by deformation. Each shell q is characterized by non-negative integer quantum numbers $q = n_x + n_y$. In each shell, there are levels depending weakly (strongly) on $V_{\rm g}$, characterized by large (small) values of n_x and small (large) values of n_y, respectively. These are referred to as "flat levels" and "steep levels", respectively. A small deviation from integrability will change the level crossings shown in Figure 2 into avoided crossings. For nearly integrable systems, the wave functions retain their character across avoided crossings. Flat levels are particularly stable, their wave functions change little with deformation (or gate voltage) and remain self-similar even after several avoided crossings [12].

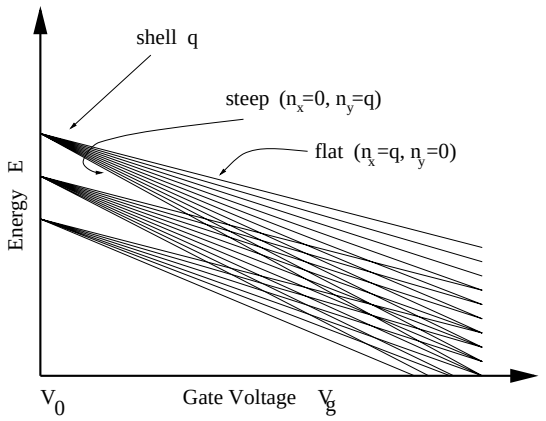

Fig. 2. Dependence of the single-particle energies of the dot on the gate voltage $V_{\rm g}$.

The matrix elements $V^{\rm L}, V^{\rm R}$ for tunneling from the left and right lead to the quantum dot are given by [16]

$$V^{\rm L(R)}(k, n_x, n_y) = \frac{\hbar^2}{2m} \int_{\rm B} {\rm d}y \left[\psi_k(x,y)^* \frac{\partial \Phi_{n_x,n_y}(x,y)}{\partial x} - \Phi_{n_x,n_y} \frac{\partial \psi_k(x,y)^*}{\partial x}\right]_{x=x_{\rm B}}. \tag{3}$$

Here $\psi_k^{\rm L(R)}$ is the wave function with wave vector k in the left (right) lead, and Φ_{n_x,n_y} is the wave function in the dot. The integration extends in the y–direction and $x_{\rm B}$ is arbitrary but must be located within the barrier [16]. We restrict ourselves to the case of a single transverse channel in each lead. The nodes of the wave functions of flat (steep) levels with large n_x (n_y) are predominantly carried by the x-component (y-component, respectively). Thus, the wave functions of flat levels extend much further into the barrier region and have considerably larger matrix elements $V^{\rm L(R)}(k, n_x, n_y)$ than those of the steep levels. This important property is illustrated in Figure 3. It has immediate consequences for the conductance at finite temperature: the very same single-particle state can dominate different Coulomb blockade resonances seen at different values of $V_{\rm g}$ [12]. We now explain this feature qualitatively, postponing a detailed discussion to later sections.

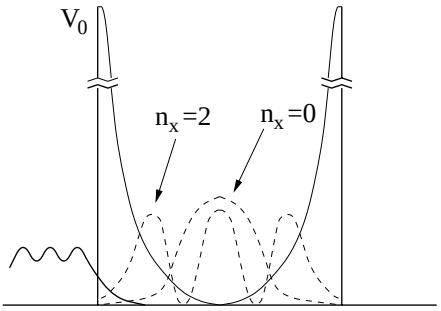

Fig. 3. The thin solid line shows a cross-section of the potential in longitudinal direction, the two barriers lying at opposite ends. The overlap of the dot wave functions (probability shown as dashed lines) and of the lead wave function (probability shown as a solid line on the left) increases strongly with the quantum number n_x in x-direction.

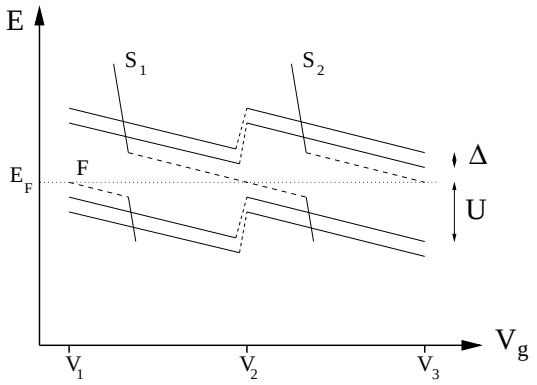

Fig. 4. Avoided crossings with the steep levels S_1 and S_2 cause the flat level F (dashed) to stay close to the Fermi energy $E_{\rm F}$. Resonances dominated by this level occur at gate voltages V_1, V_2, V_3. There is a gap of magnitude U between the last occupied and the first empty level.

At low temperature ($kT \ll \Delta$) and for small bias voltage, the transmission through the dot can be qualitatively obtained from the mean-field approximation for the dot spectrum. In this approximation, each single-particle energy ϵ_i is replaced by the effective value $\varepsilon_i = \epsilon_i + U\sum_{j\neq i}\langle n_j\rangle$ [17,18]. According to Koopmans' theorem, ε_i is the energy needed to add an electron in state i to the dot, whereas the excitation energy at fixed electron number is given by the difference of the corresponding two effective energies. Because of the Coulomb interaction, there is a gap of magnitude U between the last occupied and the first empty effective single-particle level, while the other occupied (empty) levels below (above) the Fermi energy $E_{\rm F}$ are on average separated by the usual mean level spacing Δ. Avoided crossings of single-particle levels result in avoided crossings of the effective levels, in spite of this gap [12].

A Coulomb blockade resonance occurs, and the number of electrons on the dot changes by one, whenever an effective single-particle level crosses the Fermi energy $E_{\rm F}$ of the reservoirs (we assume $E_{\rm F}$ to be independent of the gate voltage in the following). For $U \gg \Delta$, the distance between adjacent resonances is $\delta V_{\rm g} = U/\alpha$. Without level crossings, different resonances correspond to different single-particle levels. In the presence of level crossings, the situation changes. This is shown in Figure 4 which displays the gap between the filled levels below and the empty ones above $E_{\rm F}$. Resonances occur at gate voltages V_1, V_2 and V_3. Suppose a flat level F (dashed) crosses $E_{\rm F}$ at V_1. If there is an avoided crossing of F with a steep level S_1 from a higher shell between V_1 and V_2, level F is pushed above $E_{\rm F}$ while level S_1 is immersed into the Fermi sea. At V_2 the flat level F crosses $E_{\rm F}$ again, causing another resonance to occur. The mechanism works again between V_2 and V_3 where another steep level S_2 intersects with F. Since flat levels keep their wave functions after avoided crossings, the resonances at V_1, V_2 and V_3 all carry the *same* single-particle wave function. This mechanism gives rise to strong correlations of the properties (peak height and transmission phase) of several resonances. However, it leads to strong correlations only if there is *one and only one* crossing of the flat level F with a steep level within subsequent intervals $\delta V_{\rm g}$. If – on average – there is less than one (more than one) crossing, the level F will eventually be pulled down below (up above) the Fermi energy and will become irrelevant for the behavior of Coulomb blockade resonances.

It is essential for our picture for peak correlations that there be one avoided crossing with a flat level between every two successive Coulomb peaks. At finite temperature, this condition need not to be met exactly for each pair of successive peaks, but must be fulfilled on average for a sufficiently large number of pairs. We investigate this condition first within our model and later turn to the situation found experimentally. Within our model, the number of intersection points of a flat level ($n_x \neq 0, n_y = 0$) with steep levels from higher shells is found using equation (2). The total number of crossings of the flat level occurring in the range $V_{\rm g} - V_0$ is

$$N_{\rm c} = \frac{n_x^2}{2}\frac{\gamma(V_{\rm g}-V_0)}{1-\gamma(V_{\rm g}-V_0)}. \qquad (4)$$

The number of steep levels from higher shells increases with deformation and causes $N_{\rm c}$ to increase, too, until it diverges for the unphysical situation of extreme deformation $\omega_y \to 0$. One crossing within an interval $\delta V_{\rm g} = U/\alpha$ occurs for $(\partial N_{\rm c})/(\partial V_{\rm g}) = \alpha/U$. This condition yields the value $V_{\rm g}^*$ where maximal correlations between Coulomb blockade resonances are found and is used below in the calculations. We estimate the number ΔN of correlated levels as the number of resonances for which the distance between the flat level $(n_x, 0)$ and the Fermi energy is less than one level spacing. This yields

$$\Delta N \simeq 2\sqrt{n_x\sqrt{\frac{\alpha}{2\gamma U}}}, \qquad (5)$$

with a deformation $\omega_y/\omega_x = \sqrt{(\gamma U)/(2\alpha)}\ n_x$. The result (5) explicitly relates the number of correlated levels

to our model parameters. We note that ΔN sets an upper bound for the number of correlated peaks. In fact, for voltages V_g different from V_g^* the number of level crossings no longer matches the number of Coulomb peaks. In this case, the sequences of correlated peaks are shorter than ΔN. This weakens the correlations.

We have shown that within our harmonic oscillator model the condition for having on average one avoided crossing with a flat conducting level between every two successive Coulomb peaks can be met over a significant range of gate voltages. The number of correlated peaks within the model depends on the parameters α and γ which characterize the size and shape of the confining potential. Experimentally, we expect a similarly strong dependence of the peak correlations on the size and geometry of the actual quantum dot. As a result, predicting the correlations for a specific experimental setup necessarily requires the knowledge of the underlying confining potential and, hence, the solution of the corresponding electrostatic boundary-value problem. Such a calculation is beyond the scope of the present paper. Therefore, we confine ourselves to the following semiquantitative remarks. Theoretical estimates [12] have shown that for a typical setup the confining potential may indeed be well approximated by that of an anisotropic harmonic oscillator. It was also shown that near zero deformation and over a range of gate voltages, the number of level crossings may equal the number of Coulomb peaks [12]. Here we quantify these arguments.

In reference [12] a set-up with fixed barriers was considered. The authors of [12] allowed the shape of the potential to change not only in y-direction, but also in x-direction, *i.e.* $\omega_y \to \omega_y(1-\eta)$ and $\omega_x \to \omega_x(1+\eta)$. By an electrostatic estimate the deformation η could be related to the number of electrons in the dot. The change in η which occurs when another electron enters the dot is compared to the change in deformation which is necessary for two successive level crossings. Within this model we calculate the number of resonances over which a certain flat level stays within an interval of one level around the Fermi energy. We find that near zero deformation for dots containing $100-200$ electrons this condition is met for $15-25$ resonances.

We emphasize that these results do not hold generically but apply only over a specific range of gate voltages. This suggests that we cannot expect generically to find long sequences of correlated Coulomb peaks. Rather, such sequences are confined to specifically chosen flat levels. However, it must be borne in mind that the flat levels are the ones which carry by far the largest current, and thus give the strongest experimental signal. When the experimentalist adjusts the dot parameters so as to record a sequence of Coulomb peaks, he/she is more likely to pick such a level rather than one of the poorly coupled ones. This fact may lead to particularly strong correlations in experiments performed on nearly integrable dots.

So far, we have focussed attention on the resonant tunneling regime $\Gamma, kT \ll \Delta$ where only the level *at* the Fermi energy determines the properties of the resonance. Essential modifications arise for finite temperatures $kT \sim \Delta$. Here, also levels at a distance $\sim kT$ from E_F contribute to the resonance. Since the flat levels are coupled to the leads much more strongly than the steep ones, the presence of a flat level at a distance $\sim kT$ from E_F suffices for it to dominate the resonance. Long sequences of correlated resonances may occur if repeated avoided crossings cause a flat level F to stay sufficiently close to E_F over a sufficiently long range of V_g values. This is the picture we investigate quantitatively for the case of an anisotropic harmonic oscillator in the sequel. The picture suggests that the correlations of consecutive Coulomb blockade resonances will increase with temperature.

3 Coulomb blockade resonances

In this section we calculate the conductance G of a quantum dot with the single-particle spectrum (2) in linear response. We use the master equation [19]. In the Coulomb blockade regime, maxima in G occur for values of V_g where the configurations with N and $N+1$ electrons on the dot are degenerate. The resulting sharp conductance peaks are almost equally spaced [1,19]. For $kT \ll \Delta$ each peak is due to a single level n of the dot, and the peak height is given by $G \sim \Gamma_n^L \Gamma_n^R/(\Gamma_n^L + \Gamma_n^R)$ [19] with the tunneling rates $\Gamma_n^{L(R)} \sim \sum_k |V_{k,n}^{L(R)}|^2 \delta(\epsilon_n - \epsilon_k^{L(R)})$. We note that the peak heights are highly sensitive to the wave functions in the dot. Strongly coupled levels give higher peaks than the weakly coupled ones. For finite temperature several single-particle states contribute to a resonance.

Under the assumption of sequential tunneling, transport through the dot at finite temperature is described by the master equation [19]. In the regime $kT \gg \Gamma$ this equation determines the occupation probabilities P_ν of the single-particle levels of the dot under the influence of the interaction U and of the coupling to the leads. It is given by

$$\frac{\partial}{\partial t} P_\nu = \sum_{\mu(\neq\nu)} P_\mu \Gamma_{\rm in}(\mu \to \nu) - P_\nu \Gamma_{\rm out}(\nu \to \mu) \; . \quad (6)$$

Here μ and ν label Fock states, *i.e.*, Slater determinants defined in terms of the occupation numbers of all single-particle states in the dot. The symbols $\Gamma_{\rm in}$ and $\Gamma_{\rm out}$ stand for the rates of the tunneling processes into and out of the dot. These processes change the number of electrons on the dot by one, and the associated Fock states from μ to ν, and *vice versa*. The rates contain not only the coupling of the specific single-particle states of the dot to the leads but also take into account a possible suppression of tunneling by the occupation of the states in the leads. By expanding equation (6) around the equilibrium probability distribution Beenakker [19] obtained the conductance G for small bias voltage,

$$G = \frac{e^2}{kT} \sum_n \sum_{N=1}^{\infty} \frac{\Gamma_n^L \Gamma_n^R}{\Gamma_n^L + \Gamma_n^R} \; P_N^{\rm eq} \; [1 - F^{\rm eq}(\epsilon_n | N)] \times f(\epsilon_n + UN). \quad (7)$$

Table 1. Tunneling rates for several levels n calculated from equation (10). In geometry (i) the leads are opposite to each other with $\xi_x = \sqrt{50}$ and $\xi_y = 0$. In geometry (ii), the leads are arranged at an angle, with $\xi_x = \xi_y = \sqrt{50/2}$.

$n = (n_x, n_y)$	(14, 0)	(0, 14)	(6, 8)	(12, 0)	(6, 6)
Γ_n for geometry (i)	2.68×10^{-6}	4.04×10^{-23}	5.34×10^{-14}	9.09×10^{-8}	6.11×10^{-14}
Γ_n for geometry (ii)	6.30×10^{-12}	6.30×10^{-12}	5.66×10^{-7}	2.88×10^{-12}	2.41×10^{-8}

Here, f is the Fermi function and $P_N^{\rm eq}$ is the probability to find N electrons on the dot,

$$P_N^{\rm eq} = \frac{{\rm tr}_N \exp(-\beta H^{\rm D})}{{\rm tr} \exp(-\beta H^{\rm D})} = \frac{{\rm tr}_N \exp(-\beta H^{\rm D})}{\sum_N {\rm tr}_N \exp(-\beta H^{\rm D})}. \quad (8)$$

The inverse temperature is denoted by β, and ${\rm tr}_N$ denotes the trace over the Fock states with N electrons on the dot. The canonical occupation number of level n when there are N electrons on the dot is given by

$$F^{\rm eq}(\epsilon_i|N) \equiv \langle \hat{n}_i \rangle_N = \frac{{\rm tr}_N(n_i \exp(-\beta H^{\rm D}))}{{\rm tr}_N \exp(-\beta H^{\rm D})}. \quad (9)$$

Equation (7) has also been derived [20] using a Landauer-Büttiker type approach generalized to include the interaction of electrons on the dot.

Numerically, it turns out to be sufficient to calculate $F^{\rm eq}(\epsilon_n|N)$ for a window of levels around the Fermi energy, and to take the occupation numbers equal to 1 below and 0 above this window. The following results are obtained using a window of 16 levels that are populated with 8 electrons. We checked that our results are insensitive to changes of the window size.

Using equation (3) and the relation $\Gamma_n^{\rm L(R)} \sim \sum_k |V_{k,n}^{\rm L(R)}|^2 \delta(\epsilon_n - \epsilon_k^{\rm L(R)})$, we find that the tunneling rates Γ_n are proportional to the square modulus of the harmonic oscillator wave functions at the position of the barriers $\boldsymbol{r} = (x_{\rm B}, y_{\rm B})$,

$$\Gamma_n \sim \frac{(H_{n_x}(\xi_x) H_{n_y}(\xi_y))^2}{2^{(n_x+n_y)}\ n_x!\ n_y!} {\rm e}^{-(\xi_x^2+\xi_y^2)}, \quad (10)$$

where H_n are the Hermite polynomials and where we have used dimensionless variables $\xi_x = \sqrt{m\omega_x/\hbar}\ x_{\rm B}$ and $\xi_y = \sqrt{m\omega_y/\hbar}\ y_{\rm B}$. Neglecting deformation we can relate the barrier height $V_{\rm B}$ to the position of the barrier *via* $V_{\rm B}/\hbar\omega_x = (\xi_x^2 + \xi_y^2)/2$. In the sequel we choose a fixed value $V_{\rm B}/\hbar\omega = 25$ for the barrier height[2]. We consider two different geometries of the leads connecting the quantum dot with external reservoirs:

(i) the two leads are located exactly opposite to each other, so that $\xi_x = \pm\sqrt{50}$ and $\xi_y = 0$;
(ii) the leads are arranged at an angle of 90 degrees, with the barriers at $\xi_x = \xi_y = -\sqrt{50/2}$ and $\xi_x = -\xi_y = \sqrt{50/2}$.

The latter geometry has been used, for instance, in the experiment of reference [5].

The tunneling rates Γ_n for both geometries and for several states n are presented in Table 1. We note that for geometry (i) the flat levels are coupled much more strongly to the leads than the steep ones (columns 1 and 2). Comparing the rates for the flat levels of different shells we find a considerable increase with increasing n_x (columns 4 and 1). For geometry (ii) the states within one shell with equal quantum numbers n_x and n_y are most strongly coupled to the leads. However, the difference between strongly and weakly coupled states is not as pronounced as in geometry (i).

We conclude that *independently of the precise shape of the barrier*, in a geometry of type (i) which is realized in Figure 1 flat levels are more strongly coupled to the leads than steep levels. This is because the wave functions of flat levels have cigar-like shapes extending closer to the leads (*cf.* Fig. 3). Therefore, flat levels carry the bulk of the current. The difference between well coupled and poorly coupled dot states is less pronounced when the leads are arranged at an angle (geometry (ii)). In this case, the mechanism for peak correlations described in Section 2 leads us to expect a reduction in the length of sequences of correlated peaks.

We present results for $\alpha = 1$, $\gamma = 0.005$, $E_0 = -11$ and $V_0 = 90$. At zero deformation, the mean level spacing Δ is related to the harmonic oscillator frequency ω_x in x-direction by

$$\Delta = \frac{E_{\rm F}}{N_{\rm el}} = \frac{\hbar\omega_x N_{\rm sh}}{\frac{1}{2}(N_{\rm sh}+1)(N_{\rm sh}+2)} \approx \frac{2\hbar\omega_x}{N_{\rm sh}}. \quad (11)$$

Here $N_{\rm sh}$ is the number of the last filled shell and $N_{\rm el} = (N_{\rm sh}+1)(N_{\rm sh}+2)/2$ is the total number of electrons on the dot. We take $N_{\rm sh} = 14$ so that there are about 100 electrons on the dot. We assume $\Delta = 0.03U$ which roughly corresponds to the situation of the experiments of references [5,11].

In order to monitor the influence of a flat level F on the conductance, we define the distance d of F from the Fermi energy as the *number* of levels between F and the Fermi energy including F itself and count positively (negatively) for states above (below) the Fermi energy. Thus, $d = 1$ indicates that F is the first unoccupied level. Figure 5 shows

[2] Compared with typical experimental parameters this value appears to be too small. We use this value in order to avoid an unphysically large increase of Γ with increasing quantum number n_x. Such a strong increase is characteristic of the harmonically shaped barrier. A less steep increase would be obtained for steeper tunneling barriers. Such barriers appear to give a more realistic description of the depletion zone of the electron gas near the gates. For reasons of consistency with the harmonic oscillator model used throughout this paper, we decided to use harmonic barriers.

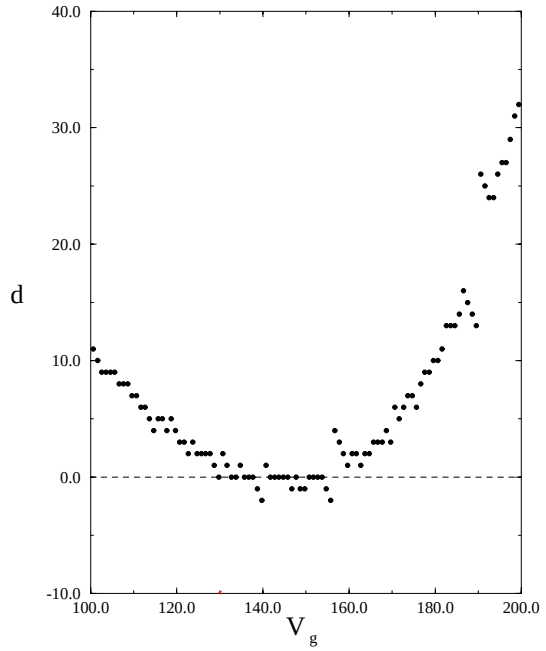

Fig. 5. Distance d (in number of levels) of the flat level ($n_x = 14, n_y = 0$) from the Fermi energy $E_{\rm F}$ *versus* gate voltage $V_{\rm g}$.

d *vs.* gate voltage for the flat level $n_x = 14, n_y = 0$. Adjacent points correspond to adjacent Coulomb blockade resonances. For $130 < V_{\rm g} < 160$, F stays in the vicinity of the Fermi energy. Hence there is – on average – one crossing with a steep level in the interval $\delta V_{\rm g}$. For $V_{\rm g} < 130$ ($V_{\rm g} > 160$), the number of avoided crossings in the interval $\delta V_{\rm g}$ is less than one (bigger than one), and F moves towards the (away from the) Fermi energy, respectively. The jumps at $V_{\rm g} = 156$ and $V_{\rm g} = 180$ are due to multiple crossings of levels which occur because of the integrability of our model.

For the same choice of parameters as in Figure 5 and for geometry (i), Figure 6 shows the conductance *vs.* gate voltage for two temperatures, $kT = 0.2\Delta$ (Fig. 6a) and $kT = 0.4\Delta$ (Fig. 6b). About 100 Coulomb blockade resonances occur in the interval $100 < V_{\rm g} < 200$. In both plots strong peaks with similar peak heights appear whenever the flat level F is close to the Fermi energy, especially at the higher temperature (Fig. 6b). In the regions $V_{\rm g} < 130$ and $V_{\rm g} > 160$ where the conductance is not dominated by the flat level F, G is much smaller than in the interval $130 < V_{\rm g} < 160$. On the scale of Figure 6, some of the conductance peaks are not even visible.

Figure 7 shows the conductance *vs.* gate voltage for the same parameters as in Figure 6b but for geometry (ii). Now, the resonances are dominated by steeper levels from higher shells which are coupled more strongly to the leads than the flat level. This is why the peak heights are bigger on average than in Figure 6, why they show stronger variation, and why they increase systematically with increasing gate voltage.

4 Phase

We now turn to the behavior of the phase of the transmission amplitude through the quantum dot. This phase has recently been measured in a set of experiments using an Aharonov-Bohm (AB) interferometer with a quantum dot embedded in one of its arms. We consider the simplest case where the AB interferometer is coupled to only one channel in each connecting lead. The transmission coefficient $\mathcal{T}$ through the AB device is then given by

$$\mathcal{T} \approx \mathcal{T}_0 + 2{\rm Re}\left\{ t_0^* {\rm e}^{-2\pi {\rm i}\Phi/\Phi_0} \int {\rm d}E \left(-\frac{\partial f}{\partial E} \right) t_{\rm QD}(E) \right\} . \quad (12)$$

Here, $\mathcal{T}_0 = |t_0|^2$ is a flux- and energy-independent term given by the square of the amplitude for transmission through the empty arm of the AB interferometer, while $t_{\rm QD}$ is the amplitude through the arm containing the dot. Since the quantum dot is weakly coupled to the arm, we have $|t_{\rm QD}| \ll |t_0|$. We have explicitly displayed the dependence on the magnetic flux Φ through the AB device and neglected higher harmonics. The symbol $\Phi_0 = h/e$ denotes the elementary flux quantum.

The master equation used in Section 3 deals with occupation probabilities and is, therefore, not able to yield the phase of the transmission amplitude $t_{\rm QD}$. We have used another approach. We have expressed $t_{\rm QD}$ in terms of the retarded Green function $G^{\rm ret}$ of the dot,

$$t_{\rm QD}(E) = \sum_{i,j} V_i^{\rm L}(E) G_{ij}^{\rm ret}(E) V_j^{\rm R*}(E) \ . \quad (13)$$

The finite-temperature Green function $G^{\rm ret}$ must be calculated in the presence of the interaction U and the tunneling. A derivation of $G^{\rm ret}$ starting from the equations of motion is given in Appendix 5. Assuming that the total number of electrons on the dot is a constant of motion, we obtain

$$G_{ij}^{\rm ret}(E) \approx \delta_{ij} \sum_{N=0}^{\infty} P_N^{\rm eq} \left[\frac{1 - \langle \hat{n}_i \rangle_N}{E - (\epsilon_i - \mu + UN) + {\rm i}\Gamma_i/2} + \frac{\langle \hat{n}_i \rangle_N}{E - (\epsilon_i - \mu + U(N-1)) + {\rm i}\Gamma_i/2} \right] . \quad (14)$$

Here $\Gamma_i = \Gamma_i^{\rm L} + \Gamma_i^{\rm R}$ and $\mu = \alpha V_{\rm g}$. The probability $P_N^{\rm eq}$ that there are N electrons on the dot and the canonical occupation number $\langle \hat{n} \rangle_N$ are given in equations (8, 9), respectively.

Within our approximations the Green function $G^{\rm ret}$ is diagonal. This fact implies that real (particle-hole) excitations of the dot caused by tunneling transitions are not taken into account. This is justified in the regime of elastic cotunneling $kT < \sqrt{U\Delta}$ where inelastic cotunneling processes do not contribute significantly to the transmission [2]. Equation (14) is a good approximation to the exact retarded Green function between Coulomb blockade resonances where fluctuations in the occupation number of the dot are strongly suppressed. Moreover, *even at resonance* where $G^{\rm ret}$ reduces to a single Breit-Wigner term, equation (14) is expected [21] to apply provided there are no

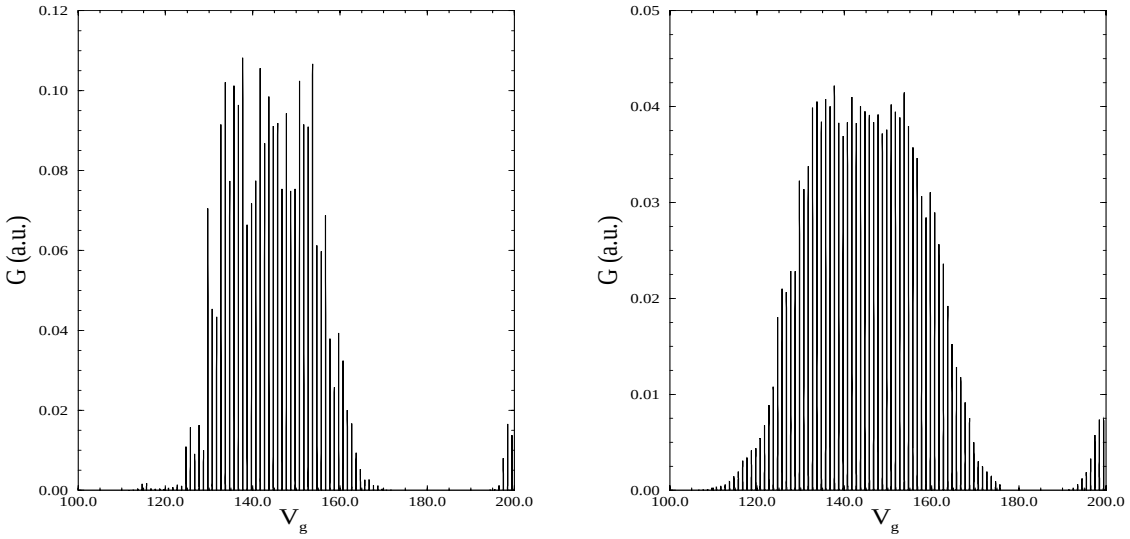

Fig. 6. Conductance G *vs.* gate voltage for (a) $kT = \Delta/5$ and (b) $kT = 2\Delta/5$.

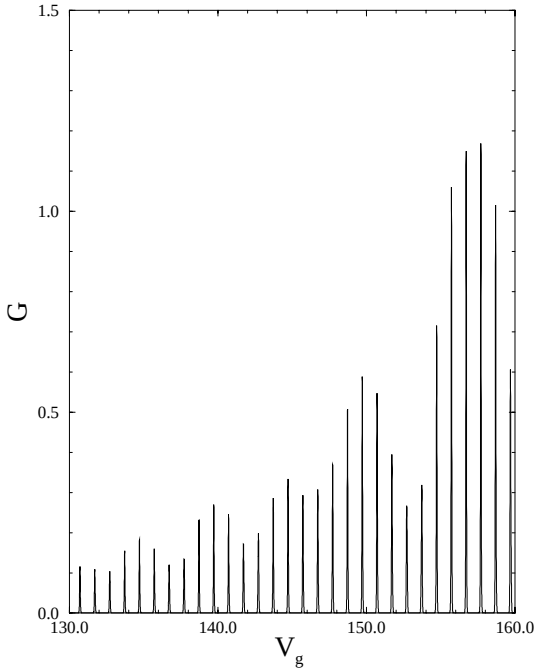

Fig. 7. Conductance G *vs.* gate voltage $V_{\rm g}$ for the same parameters as in Figure 6b but with the leads arranged at an angle of 90 degrees.

degeneracies and we work well above the Kondo temperature [22]. The success of equation (14) in these limiting cases suggests that well above the Kondo temperature, equation (14) is a good approximation to the exact Green function for all energies.

Combining equations (14, 12) we obtain

$$\mathcal{T} = \mathcal{T}_0 + \mathrm{Re}\; t_0^*\; \widetilde{t_{\rm QD}}\; \mathrm{e}^{-2\pi \mathrm{i}\Phi/\Phi_0}, \qquad (15)$$

where

$$\begin{aligned}\widetilde{t_{\rm QD}} &= \int \mathrm{d}E \left(-\frac{\partial f}{\partial E}\right) t_{\rm QD}(E) \\ &= \frac{\beta}{2\pi\mathrm{i}} \sum_i \sum_{N=0}^{\infty} V_i^{\rm L} V_i^{\rm R*} P_N^{\rm eq} \\ &\quad \times \left[(1-\langle \hat{n}_i\rangle)\psi^{(1)}\left(\frac{\beta}{2\pi\mathrm{i}}(\mathrm{i}\Gamma_i - \epsilon_i + \mu - UN) + \frac{1}{2}\right)\right. \\ &\quad \left. + \langle \hat{n}_i\rangle \psi^{(1)}\left(\frac{\beta}{2\pi\mathrm{i}}(\mathrm{i}\Gamma_i - \epsilon_i + \mu - U(N-1)) + \frac{1}{2}\right)\right] \qquad (16)\end{aligned}$$

with the trigamma function $\psi^{(1)}$.

In Figure 8 we show the phase ϕ of the transmission amplitude versus gate voltage. As in the calculation of the conductance in Section 3, the canonical occupation numbers are obtained by distributing 8 electrons over a window containing 16 levels. We take $\Gamma_i = \Gamma = 0.002U = \Delta/15$. The solid lines at the bottom of the plots show the conductance peaks and help to identify the resonance positions. In the left part of Figure 8 the flat level $n_x = 14$, $n_y = 0$ is close to the Fermi energy. Here we find a strikingly similar behavior of the phase at all resonances. This behavior is found not only within the $V_{\rm g}$ interval shown but *for the entire interval* $130 < V_{\rm g} < 160$ *comprising 30 resonances.* The phase regularly increases by π at resonance and displays a sharp lapse by π between adjacent resonances. As observed in references [13,14] the increase at resonance occurs on the scale kT (we assume $kT > \Gamma$) and the phase lapse between resonances on the scale Γ. The temperature dependence of the phase is shown in Figure 9. In the right part of Figure 8 we show the transmission phase for the case where the distance between the flat level and the Fermi energy is large compared to kT and increases with $V_{\rm g}$ (*cf.* Fig. 5). The phase behaves less regularly, with an increase by π or less

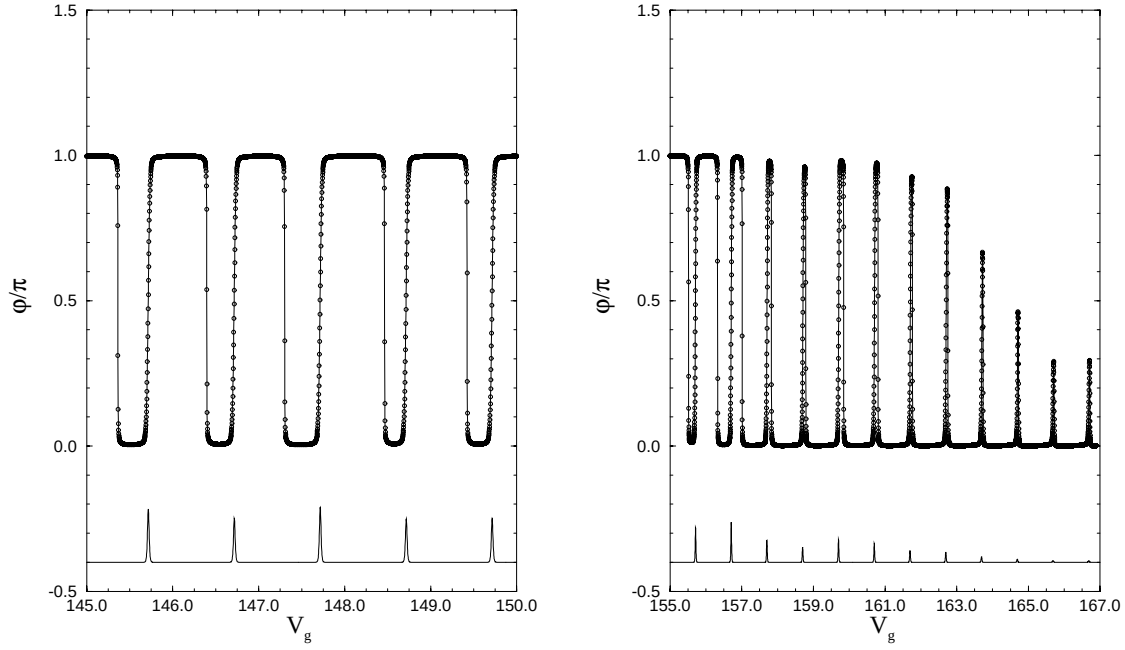

Fig. 8. Phase ϕ of the transmission amplitude *versus* gate voltage $V_{\rm g}$ at $kT = \Delta/5$ in two different intervals. The solid lines at the bottom of the plots display the conductance peaks. In the case shown in the left (right) part, the flat level $n_x = 14, n_y = 0$ is at or near (far removed from) the Fermi level, respectively. In the case of the right part, the flat level influences the phase as a background only.

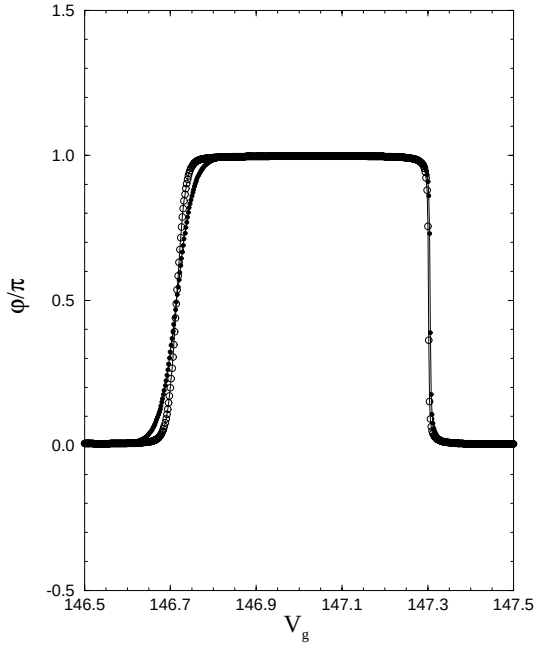

Fig. 9. Transmission phase for $kT = 0.2\Delta$ (open circles) and $kT = 0.4\Delta$ (filled circle). The increase by π at the resonance takes place on the scale kT, the phase lapse between resonances, on the scale Γ.

at and an immediate phase lapse near the resonances. Between resonances the phase remains virtually constant.

To interpret our results, we consider first the phase ϕ at resonance. The identical behavior of ϕ at all resonances in Figure 8a reflects the fact that at each resonance, the transmission through the dot is dominated by the strongly coupled level F. This is the same mechanism as in the sequence of strong conductance peaks shown in Figure 6a. The more erratic phase behavior seen in Figure 8b is the result of the interplay of various levels of the dot. The regular behavior of the phase lapse between adjacent resonances is also due to the dominance of the flat level. At finite temperature the flat level F has a finite probability of being either occupied or empty and, thus, may contribute to both an electron-like and a hole-like cotunneling process. The contribution of both processes to the transmission amplitude through the dot is

$$t_{\rm F} = V_{\rm F}^{\rm L} V_{\rm F}^{\rm R*} \left[\frac{1 - \langle \hat{n}_{\rm F} \rangle_N}{E - (\epsilon_{\rm F} - \mu + UN) + {\rm i}\Gamma_{\rm F}/2} + \frac{\langle \hat{n}_{\rm F} \rangle_N}{E - (\epsilon_{\rm F} - \mu + U(N-1)) + {\rm i}\Gamma_{\rm F}/2} \right] \quad (17)$$

where the first (second) term represents the electron-like (hole-like) contribution, respectively. As the gate voltage $V_{\rm g} = \mu/\alpha$ scans the Nth valley (*i.e.* varies from $(\epsilon_N + U(N-1))/\alpha$ to $(\epsilon_{N+1} + UN)/\alpha$), the sign of Re $t_{\rm F}$ reverses, leading to a phase lapse. The same conclusion has previously been reached in reference [13]; an interpretation in terms of scattering theory has been given in reference [14]. If F is far away from the Fermi energy (on the scale of kT) either the particle-like or the hole-like process will dominate, and the phase lapse moves from the valley towards the resonance, as depicted in Figure 8b.

We emphasize that the phase lapse between resonances is a genuine interaction effect. Indeed, the interaction U is needed to keep the flat level close to the Fermi energy for a long sequence of resonances. For non-interacting particles ($U \to 0$) the transmission amplitude at different resonances would be dominated by different single-particle levels. In the same limit, the cotunneling amplitude (17) would reduce to a single, temperature-independent term. The phases of the transmission amplitude in consecutive valleys would not be correlated, and there would be no systematic phase lapse between resonances. We also note that the systematic phase lapse occurs only at finite temperature. At zero temperature a flat level could only contribute to either particle-like or hole-like cotunneling.

5 Summary – The question of non-universality

Since the first measurements on quantum dots in Aharonov-Bohm interference devices were reported, many aspects of phase-coherent transport through quantum dots have been understood theoretically. However, one of the most striking features, the strong correlations of the transmission phases in sequences of many resonances, has long withstood a satisfactory theoretical explanation. Earlier attempts [13] to solve the problem could account for short sequences but not for the sequences of more than 10 resonances found experimentally.

In this paper we have demonstrated the viability of a mechanism, based on a synthesis of the ideas proposed in references [12,13], that gives rise to long sequences of correlated peak heights and transmission phases. We have used several approximations, the most central one being that the confining potential defining the dot is "almost" integrable. More precisely, both the deviation from integrability and the disorder must constitute a perturbation which is small on the scale of the mean single-particle level spacing. Regarding the experiments of reference [11], we do not know whether the quantum dots used do obey this condition, and whether one avoided crossing per added electron did occur on average. If this were indeed the case, our model might account semiquantitatively for the phase correlations observed in these experiments. Nevertheless, our analysis naturally falls short of providing a complete and universal framework which could account for the combined effect of disorder and interaction on correlations in transmission experiments.

We have used the following specific conditions and assumptions.

(i) Among the eigenstates of the quantum dot, some must be coupled more strongly to the leads than others. This assumption is met by a model which is nearly integrable, as is the case for our parabolic confining potential. This potential renders (n_x, n_y) good quantum numbers for all values of V_g. Of all levels in a shell, the level with $n_y = 0$ is most strongly coupled to the leads.

(ii) Changes in the gate voltage induce deformations of the dot boundary such that the potential is deformed in the transverse y-direction. This assumption guarantees that in each shell, the level with $n_y = 0$ is flat, *i.e.*, stays close to the Fermi energy over a wide range of V_g-values.

(iii) On average there is one crossing of the flat level with one other level per unit interval. This interval is defined by the change in V_g needed to add an extra electron to the dot.

(iv) The temperature is sufficiently high to produce sufficiently long sequences of correlated resonances. The minimum temperature required by this condition depends both on the distance of the most strongly coupled level from the Fermi energy, and on the relative strength of the coupling of that level to the leads. With increasing temperature the correlations become more robust.

Strong boundary deformations leading to strongly chaotic classical motion within the dot, or strong disorder in the dot are likely to destroy the correlations altogether since they generically do not allow for the existence of eigenstates that are particularly well coupled to external leads. In this sense, the correlations proposed in the present paper are *non-universal in origin*.

Our ideas may be checked experimentally on dots that are not embedded in an AB device but are coupled directly to leads. This setup does not allow for tests of phase correlations but provides a convenient setup for measuring conductance peak correlations. The conductance of a dot with a regular (rectangular) lithographic shape has been measured by Simmel *et al.* [23]. These authors did indeed find a sequence of more than 10 strong peaks with very similar peak heights. In the same sweep they also observe envelopes of smaller peaks very similar to our results in Figure 6. To test our picture further, it would be illuminating to perform a similar two-terminal conductance experiment with leads attached at two sides of the dot which form an angle of 90 degrees. Here, a reduction of the correlations is to be expected. It would also be interesting to compare two setups, one with a plunger gate and the other with a backgate configuration. In the latter case the potential deformation is reduced. This should suppress our correlation mechanism.

This work was supported by the German-Israeli Foundation (GIF), by the Israel Science Foundation founded by the Israel Academy of Sciences and Humanities-Centers of Excellence Program, and by the U.S.-Israel Binational Science Foundation (BSF).

Appendix A: Retarded Green function

We derive equation (14). The retarded Green function is defined as

$$G^{\mathrm{ret}}_{kl} = -\mathrm{i}\theta(t)\ \langle [c_k(t), c^\dagger_l(0)]_+ \rangle = F_{kl} + G_{kl} \qquad \text{(A.1)}$$

where

$$G_{kl} = -\mathrm{i}\theta(t)\langle c_k(t)c_l^\dagger(0)\rangle \quad F_{kl} = -\mathrm{i}\theta(t)\langle c_l^\dagger(0)c_k(t)\rangle. \quad \text{(A.2)}$$

The brackets denote the thermal average, $\langle ...\rangle = \mathrm{tr}(... \exp(-\beta H))/\mathrm{tr}(\exp(-\beta H))$.
With $P_N = \mathrm{tr}_N \exp(-\beta H)/\mathrm{tr}\exp(-\beta H)$, we write the trace as a sum of terms with a fixed number N of electrons on the dot,

$$G_{kl} = -\mathrm{i}\theta(t)\sum_{N=0}^{\infty} P_N\langle c_k(t)c_l^\dagger(0)\rangle_N = \sum_{N=0}^{\infty} G_{kl}^{(N)} \ . \quad \text{(A.3)}$$

In the "equation of motion" method the Green function is differentiated with respect to time. Since the time evolution of an operator is given by the commutator with the Hamiltonian, a system of differential equations containing higher-order Green functions is generated. A closed system is obtained if these Green functions can be approximately uncoupled. The solution is obtained by Fourier transformation. Specifically,

$$\frac{\partial}{\partial t}G_{ij}^{(N)} = -\mathrm{i}\delta(t)\langle c_i(0)c_j^\dagger(0)\rangle_N - \theta(t)\langle [c_i, H](t)c_j^\dagger(0)\rangle_N \quad \text{(A.4)}$$

$$\begin{aligned} &= -\mathrm{i}\delta(t)\langle c_i(0)c_j^\dagger(0)\rangle_N \\ &\quad - \theta(t)\Big((\epsilon_i-\mu)\langle c_i(t)c_j^\dagger(0)\rangle_N + U\langle N(t)c_i(t)c_j^\dagger(0)\rangle_N\Big) \\ &\quad - \theta(t)\sum_k \Big(V_{ki}^{\mathrm{L}*}\langle a_k(t)^{\mathrm{L}}c_j^\dagger(0)\rangle_N + V_{ki}^{\mathrm{R}*}\langle a_k(t)^{\mathrm{R}}c_j^\dagger(0)\rangle_N\Big). \end{aligned} \quad \text{(A.5)}$$

Since the interaction contains two creation and two annihilation operators a two particle Green function appears in the second line. The last two terms stem from the coupling to the leads, and by another equation of motion can be expressed in terms of the Green function for the dot. Assuming that the states in the lead and in the dot are uncorrelated at $t = 0$ we obtain

$$\langle a_k(t)c_j^\dagger(0)\rangle_N = \sum_i V_{ki}^{\mathrm{L}}\int \mathrm{d}\bar{t}\, G_{ij}^{(N)}(t-\bar{t})\theta(\bar{t})\exp(-\mathrm{i}\epsilon_k^{\mathrm{L}}\bar{t}). \quad \text{(A.6)}$$

Fourier transformation of equation (A.5) yields

$$\begin{aligned} \omega G_{ij}^{(N)} &= \langle 1-n_i\rangle_N\delta_{ij} + (\epsilon_i-\mu)G_{ij}^{(N)} + U\tilde{G_{ij}} \\ &\quad + \sum_{kl}\left(\frac{V_{ki}^{\mathrm{L}*}V_{kl}^{\mathrm{L}}}{\omega-\epsilon_k^{\mathrm{L}}+\mathrm{i}\delta} + \frac{V_{ki}^{\mathrm{R}*}V_{kl}^{\mathrm{R}}}{\omega-\epsilon_k^{\mathrm{R}}+\mathrm{i}\delta}\right)G_{lj}^{(N)} \end{aligned} \quad \text{(A.7)}$$

where $\tilde{G_{ij}} = -\mathrm{i}\int \mathrm{d}t\theta(t)\langle N(t)c_i(t)c_j^\dagger\rangle_N \exp \mathrm{i}\omega t$. The equations of motion are closed by assuming the total occupation N to be constant. Then the number operator can be taken out of the expectation value. The assumption is justified in the valleys between resonances whereas at each resonance, N fluctuates. For isolated resonances (level width $\ll$ level spacing), we have $\mathrm{Im}\sum_k V_{ki}^{\mathrm{L}*}V_{kl}^{\mathrm{L}}/(\omega-\epsilon_k^{\mathrm{L}}+\mathrm{i}\delta) = -\mathrm{i}\delta_{il}\Gamma_i^{\mathrm{L}}/2$. This yields

$$G_{ij}^{(N)} = \frac{\delta_{ij}\langle 1-n_i\rangle_N}{\omega-(\epsilon_i-\mu+UN)+\mathrm{i}\Gamma_i^{\mathrm{L}}/2+\mathrm{i}\Gamma_i^{\mathrm{R}}/2}. \quad \text{(A.8)}$$

For F_{ij} we proceed analogously and eventually obtain equation (14).

References

1. L.P. Kouwenhoven, C.M. Marcus, P.L. McEuen, S. Tarucha, R.M. Westervelt, N.S. Wingreen, *Proceedings of the NATO Advanced Study Institute on Mesoscopic Electron Transport*, edited by L.P. Kouwenhoven, L. Sohn, G. Schön (Kluwer Series E, 1997).
2. D.V. Averin, Yu.N. Nazarov, Phys. Rev. Lett. **76**, 1695 (1990).
3. R. Jalabert, A.D. Stone, Y. Alhassid, Phys. Rev. Lett. **68**, 3468 (1992).
4. A.M. Chang, H.U. Baranger, L.N. Pfeiffer, K.W. West, T.Y. Chang, Phys. Rev. Lett. **76**, 1695 (1996).
5. J.A. Folk, S.R. Patel, S.F. Godijin, A.G. Huibers, S.M. Cronenwett, C.M. Marcus, Phys. Rev. Lett. **76**, 1699 (1996).
6. U. Sivan, R. Berkovits, Y. Aloni, O. Prus, A. Auerbach, G. Ben-Yoseph, Phys. Rev. Lett. **77**, 1123 (1996).
7. Y. Alhassid, M. Gökcedag, A.D. Stone, Phys. Rev. B **58**, R7524 (1998).
8. R. Berkovits, U. Sivan, Europhys. Lett. **41**, 653 (1998).
9. R.O. Vallejos, C.H. Lewenkopf, E.R. Mucciolo, Phys. Rev. Lett. **81**, 677 (1998).
10. S.R. Patel, D.R. Stewart, C.M. Marcus, M. Gökcedag, Y. Alhassid, A.D. Stone, C.I. Duruöz, J.S. Harris Jr., Phys. Rev. Lett. **81**, 5900 (1998).
11. R. Schuster, E. Buks, M. Heiblum, D. Mahalu, V. Umansky, H. Shtrikman, Nature **385**, 417 (1997).
12. G. Hackenbroich, W.D. Heiss, H.A. Weidenmüller, Phys. Rev. Lett. **79**, 127 (1997).
13. Y. Oreg, Y. Gefen, Phys. Rev. B **55**, 13726 (1997).
14. G. Hackenbroich, H.A. Weidenmüller, Europhys. Lett. **38**, 129 (1997).
15. L. Brey, N.F. Johnson, B.I. Halperin, Phys. Rev. B **40**, 10647 (1989); S.K. Yip, Phys. Rev. B **43**, 1707 (1991); Q.P. Lie, K. Karrai, S.K. Yip, S. Das Sarma, H.D. Drew, Phys. Rev. B **43**, 5151 (1991); W.D. Heiss, R.G. Nazmitdinov, Phys. Rev. B. **55**, 16310 (1997).
16. C.B. Duke, *Tunneling in Solids*, Solid State Physics Suppl. **10**, edited by F. Seitz, D. Turnbull, H. Ehrenreich (Academic Press, 1969).
17. P.W. Anderson, Phys. Rev. **124**, 41 (1961).
18. G. Hackenbroich, H.A. Weidenmüller, Phys. Rev. B **53**, 16379 (1996).
19. C.W.J. Beenakker, Phys. Rev. B **44**, 1646 (1991).
20. Y. Meir, N.S. Wingreen, P.A. Lee, Phys. Rev. Lett. **66**, 3048 (1991).
21. C.A. Stafford, Phys. Rev. Lett. **77**, 2770 (1996).
22. L.I. Glazman, M.E. Raikh, Pis'ma Zh. Eksp. Teor. Fiz. **47**, 378 (1988) [JETP Lett. **47**, 452 (1988)]; H. Schoeller, G. Schön, Phys. Rev. B **50**, 18436 (1994); A. Kamenev, Y. Gefen, Phys. Rev. B **54**, 5428 (1996).
23. F. Simmel, T. Heinzel, D.A. Wharam, Europhys. Lett. **38**, 123 (1997).